

# A novel cytoplasmic interaction between junctin and ryanodine receptor calcium release channels.

by

Linwei Li, Shamaruh Mirza, Spencer J. Richardson, Esther M. Gallant, Chris Thekkedam, Suzy M. Pace, Francesco Zorzatto, Dan Liu, Nicole A. Beard<sup>#</sup> and Angela F. Dulhunty<sup>#</sup>

John Curtin School of Medical Research, ACT, Australia, 0200

<sup>#</sup>equal senior author contribution

**Corresponding Author:** Prof AF. Dulhunty  
John Curtin School of Medical Research  
Australian National University,  
PO Box 334,  
Canberra, ACT 2601  
Australia  
Telephone +61 2 6125 4491  
Fax +61 2 6125 4761  
Email [angela.dulhunty@anu.edu.au](mailto:angela.dulhunty@anu.edu.au)

**Running title:** Junctin and ryanodine receptors.

## **Abstract**

Junctin, a non-catalytic splice variant of the aspartate- $\beta$ -hydroxylase gene, is inserted into the membrane of the sarcoplasmic reticulum (SR)  $\text{Ca}^{2+}$  store where it modifies  $\text{Ca}^{2+}$  signalling in the heart and skeletal muscle through its regulation of ryanodine receptor (RyR)  $\text{Ca}^{2+}$  release channels. Junctin is required for normal muscle function as its knockout leads to abnormal  $\text{Ca}^{2+}$  signalling, muscle dysfunction and cardiac arrhythmia. However, junctin's binding interactions with RyRs are largely unknown and have been assumed to occur only in the SR lumen. We find robust binding of RyRs to full junctin, its luminal and unexpectedly its cytoplasmic domain, each with distinct effects on RyR1 and RyR2 activity. Full junctin in the luminal solution increases channel activity by ~3-fold. The C-terminal luminal interaction inhibits RyR channel activity by ~50%. The N-terminal cytoplasmic binding produces a ~5-fold increase in RyR activity. The cytoplasmic interaction is required for luminal binding to replicate the influence of full junctin on RyR1 and RyR2 activity. The C-terminal domain of junctin binds to residues including S1-S2 linker of RyR1 and N-terminal junctin binds between RyR1 residues 1078-2156.

**Key words:** junctin, skeletal and cardiac ryanodine receptors, sarcoplasmic reticulum, cytoplasmic interaction, luminal interaction.

## **Introduction**

Contraction in the heart and skeletal muscle depends on the release of  $\text{Ca}^{2+}$  from the intracellular sarcoplasmic reticulum (SR)  $\text{Ca}^{2+}$  store. Inherited or acquired changes in  $\text{Ca}^{2+}$  release lead to skeletal and cardio-myopathies and cardiac death (Gyorke and Carnes, 2008). The efficacy of  $\text{Ca}^{2+}$  release depends on an influence of the “ $\text{Ca}^{2+}$  load” in the SR on the activity of ryanodine receptor (RyR)  $\text{Ca}^{2+}$  release channels, which is facilitated by a  $\text{Ca}^{2+}$ -dependent interaction between CSQ and the RyR via the “anchoring” protein junctin (Dulhunty et al., 2009; Dulhunty et al., 2012; Wei et al., 2009a). A second “anchoring” protein, triadin also binds to CSQ and the RyR, but does not transmit signals from CSQ to the RyR in skeletal muscle *in vitro* (Wei et al., 2009a), although it does influence  $\text{Ca}^{2+}$  release during excitation-contraction (EC) coupling in intact myotubes (Goonasekera et al., 2007) and anchoring of CSQ to the junctional SR membrane (Boncompagni et al., 2012). Different isoforms of the RyR, CSQ and triadin are expressed in cardiac and skeletal muscle, whilst the same isoform of junctin is expressed in both muscle types.

The functions of junctin, triadin and CSQ in SR  $\text{Ca}^{2+}$  signalling have been extensively explored in transgenic animals. Triadin-, junctin-, or CSQ-null animals survive, but their longevity and ability to tolerate stress is compromised (Altschafel et al., 2011; Dainese et al., 2009; Oddoux et al., 2009). Thus normal expression of each of the proteins is required for normal function. In contrast to the transgenic studies there are few reports addressing molecular interactions between either triadin or junctin and the RyR *in vitro*. The regions of junctin that support functional interactions with RyRs are unknown. Junctin contains a short N-terminal cytoplasmic domain, a single SR membrane spanning domain and a longer luminal C-terminal domain (Fig. 1A) that contains binding sites for CSQ and the RyR (Altschafel et al., 2011; Kobayashi et al., 2000). The binding site for junctin on RyR1 has not been determined, but two junctin-binding regions on luminal domains of RyR2 have been identified (Altschafel et al., 2011). Our aim here has been to examine functional interactions between junctin and skeletal RyR1 and cardiac RyR2 channels and to explore the role of the cytoplasmic and luminal domains of junctin in modulating RyR activity. The results show the expected interaction between the luminal domain of junctin (as well as one of its KEKE-like motifs) with luminal but not cytoplasmic domains of RyR1 and RyR2 channels. In addition we find an unexpected and robust interaction between the cytoplasmic domain of junctin and cytoplasmic, but not luminal, domains of RyR1 and RyR2. The cytoplasmic interaction appears essential to reproduce the effect of full junctin on the RyR channels.

## **Results**

**Full length junctin, its C-terminal and N-terminal domains bind to RyR1 and RyR2.** Complex immunoprecipitation (co-IP) and affinity chromatography were used to determine junctin's association with RyRs. RyR2 purified from sheep heart or RyR1 from rabbit skeletal muscle were coupled to anti-RyR1 protein A/G agarose and full length junctin (FLjun; isolated from skeletal muscle) or C-terminal domain of canine junctin (Cjun, expressed in *E. coli*) coupled to anti-junctin protein A/G agarose, to assess binding to RyRs. FLjun bound to both RyR2 and RyR1 using anti-junctin co-IP (Fig. 1C lanes 1 and 2), or when RyRs were conjugated with anti-RyR protein A/G agarose (n=2-3, included in averages in Fig. 1D). There was similar association between Cjun and RyR2 or RyR1, using both anti-RyR (Fig. 1C, lanes 3 and 4) and anti-jun co-IP (n=2-3, included in averages in Fig. 1D). Comparable amounts of Cjun and FLjun bound to the RyRs (Fig. 1D). The density of RyR2 bands was lower than RyR1 due to reduced antibody affinity for RyR2. Neither FLjun, Cjun, RyR1 or RyR2 associated with protein A/G agarose in the absence of antibody or in the presence of antibody, but absence of epitope (e.g. Fig. 1C, lanes 5 and 6).

As it was assumed that the RyR interactions with junctin occur only between the luminal domains of the proteins, it was surprising that RyR1 and RyR2 bound to the biotinylated Njun peptide (Fig. 1E, lanes 2 and 5). Since RyRs isolated from heart or skeletal muscle bound to NeutrAvidin agarose beads, but recombinant RyR1 and RyR2 did not (Fig. 1E, lanes 1 and 4), recombinant channels were used in this experiment. However a similar interaction between muscle-isolated RyRs and the cytoplasmic domain of Njun is supported by the functional and binding data described below. Some RyR bound to the scrambled Njun peptide (Fig. 1E, lanes 3 and 6), but this was <20% of that bound by Njun (Fig. 1F). Neither adding 1% triton X-100 to the wash buffer, nor increasing the volume of wash buffer or number of washes, altered the binding. This limited binding was considered either non-specific or non-functional as the scrambled peptide did not alter channel activity (Fig. 3 below). It is perhaps not surprising that scrambled Njun (with a PI of 9.70, containing 2E, 3K and 2H) associated weakly and non-specifically with RyRs, without functional consequences, as the large cytoplasmic domain of the RyR contains hydrophilic surfaces. Attempts at complimentary Co-IP of Njun by RyRs was unsuccessful as the Njun peptide bound to A/G agarose (n=4).

**Full length junctin activates RyR2 and RyR1 channels from heart and skeletal muscle.** RyR channels added to the *cis* solution incorporate into bilayers with their cytoplasmic side facing that solution and luminal side facing the *trans* solution (Beard et al., 2002; Laver, 2005). Therefore these solutions are referred to as cytoplasmic and luminal respectively. The average conductances were  $284.8 \pm 9.1$  pS for RyR1 or  $266.6 \pm 10.5$  for RyR2 in the range reported previously with physiological

[Ca<sup>2+</sup>]s of 1 μM *cis* and 1 mM *trans* (Laver et al., 1995; Tinker and Williams, 1993; Wei et al., 2009a). Channel activity increased when FLjun was added to the luminal solution at a maximal activating concentration of 213 nM (molar equivalent of 5 μg/ml used previously (Wei et al., 2009a)) (Fig. 2A-C), associated with an increase in mean open time and decrease in mean closed time (Fig. 2D&E). The open and closed time distributions were described by three time constants that were not altered by FLjun, although there was a significant increase in long openings in  $\tau_{o3}$  (and fewer in  $\tau_{o1}$ ), and a decrease in long closures in  $\tau_{c3}$  (with more in  $\tau_{c1}$ ) (Fig. 2F&G).

In control experiments, FLjun was added to the luminal side of native RyR channels containing endogenous junctin (see Fig. 4 below and (Wei et al., 2009a)). The rationale was that if endogenous junctin was bound to native RyRs, then exogenous FLjun added to the luminal solution could not bind to or activate the channels. Consistently, there was no significant effect of luminal FLjun on either native RyR1 or native RyR2 channels (Fig 2H).

**The N-terminal domain of junctin activates RyR channels.** Njun added to the cytoplasmic solution dramatically increased RyR activity (Fig. 3A&B). RyR2 open probability increased 6.9±2.4-fold and RyR1 increased 5.0±1.0-fold (Fig. 3C). This was significantly greater than the 2.8±0.44 (RyR2, p=1.2E-03) and 1.9±0.14 (RyR1, p=1.9E-04) increases produced by luminal FLjun, but was similarly due to longer open times (Fig. 3D) and briefer closures (Fig. 3E). As with FLjun, there was no change in open or closed time constant values, but a decrease in the number of longest closed events and increase in the number of longest opening events (Fig. 3G&H). Channel activity was not altered by cytoplasmic Njun<sub>scrambled</sub> (Fig. 3F) or by luminal Njun (Fig. 3I), indicating a specific action of Njun on the cytoplasmic side of the RyRs.

To indicate whether Njun was bound to RyR1 *in vivo*, we again utilised native RyR channels in SR vesicles containing endogenous junctin. As with FLjun, the rationale was that if the N-terminal domain of endogenous junctin was bound to native RyRs, then exogenous Njun added to the cytoplasmic solution could not bind to the channels. Indeed there was no significant change in relative gating parameters after adding 213 nM Njun to the cytoplasmic side of native RyRs incorporated with SR vesicles (Fig. 3J-L). We also examined effects of Njun on Ca<sup>2+</sup> release from SR vesicles, through native RyRs which are oriented with their cytoplasmic surface facing the extravesicular solution (Saito et al., 1984). Njun was added at 5 μM because high peptide concentrations are required to instantly alter Ca<sup>2+</sup> release from SR (Dulhunty et al., 1999). Consistent with single channel results, Njun did not immediately alter resting Ca<sup>2+</sup> release from cardiac or skeletal SR (Fig. 3M left). Similarly, 20 min pre-incubation in 5 μM Njun (plus 10 min exposure during Ca<sup>2+</sup> loading steps) did not alter caffeine-induced Ca<sup>2+</sup> release (Fig. 3M right),

which reflects the physiological  $\text{Ca}^{2+}$ -induced  $\text{Ca}^{2+}$  release process (Pagala and Taylor, 1998).

Therefore we suggest that most Njun binding sites are occupied by the N-terminal tail of endogenous junctin and thus that Njun binding to RyRs may occur *in vivo*.

**The C-terminal domain of junctin inhibits RyR channels.** We expected that luminal Cjun would activate RyRs in the same way as FLjun, due to an assumed dominance of the luminal interaction between the proteins. Contrary to expectation Cjun inhibited the channels (Fig. 4A-C, solid black bins).  $P_o$  fell to  $0.48 \pm 0.06$  of control in RyR2 and to  $0.68 \pm 0.17$  in RyR1, due to a small abbreviation of open times (Fig. 4D) and a larger increase in closed times (Fig. 4E). The open and closed time constants were not affected by Cjun, but there were fewer long open events and more long closed events (Fig. 4F&G). This was likely to be a specific effect of the native Cjun because denaturing the protein by boiling for 10 min removed its effects on channel open probability (Fig. 4H).

Cjun added to the cytoplasmic (*cis*) solution caused a small significant decline in channel activity (Fig. 4C-E, narrow cross-hatched bins), that was significantly less than the fall in activity with Cjun in the luminal solution (RyR2,  $p=1.8\text{E-}03$ ; RyR1,  $p=0.047$ ). This was not due Cjun crossing the bilayer to access luminal RyR domains, as subsequent addition of luminal Cjun produced normal inhibition and, conversely, luminal addition of Cjun did not prevent the effect of subsequent cytoplasmic addition ( $n=6$ , RyR1 and  $n=12$ , RyR2). To determine whether C-terminal domain of endogenous junctin bound to the cytoplasmic side of native RyRs, cytoplasmic Cjun was added to native channels where it inhibited RyR2 but not RyR1 (Fig. 4C-E, wide hatched bins). In contrast however, the rate of  $\text{Ca}^{2+}$  release from SR vesicles was unaffected by  $5 \mu\text{M}$  Cjun either immediately after addition or during caffeine-induced  $\text{Ca}^{2+}$  release after 20 min pre-incubation plus 10 min exposure during  $\text{Ca}^{2+}$  loading (Fig. 4I). Finally, recombinant FLjun with a his-tag protected N-terminus added to the cytoplasmic side of purified channels, did not consistently change gating (Fig. 4C-E, grey bins). These inconsistent results suggest that any cytoplasmic effect of Cjun is weak and non-specific. As with scrambled Njun, this is not surprising given the overall highly charged nature of both Cjun and cytoplasmic RyR domains.

The strong action of Cjun on the luminal side of purified RyRs was not due the peptide binding to residual CSQ associated with the solubilised RyR as there is no detectable CSQ, triadin or junctin in these preparations (Fig 4J-L).

**Combined actions of Cjun and Njun on RyR channels.** Since junctin appears to regulate RyRs through its N- and C-terminal domains, we examined the combined effect of cytoplasmic Njun plus luminal Cjun. Njun added first to the cytoplasmic solution increased activity (1<sup>st</sup> black bin, Fig. 5A-F) to levels significantly greater than luminal FLjun (cross-hatched bins). Subsequent luminal

addition of Cjun reduced the open probability (2<sup>nd</sup> black bin), to levels that remained greater than control, but were not significantly different from those with luminal FLjun.

In the complementary experiment,  $P_o$  fell when luminal Cjun was added first and then increased with cytoplasmic Njun addition, but remained less than control (grey bins, Fig. 5A-F). This was in contrast to greater than control activity with cytoplasmic Njun alone (Fig. 5 black bins and Fig. 3 above) or with luminal FLjun (cross-hatched bins). Similar changes in open probability with FLjun (luminal), or Njun (cytoplasmic) followed by Cjun (luminal), were mainly due to changes in closed times (red ovals Fig. 5C&F). These results suggest that increased RyR activity with luminal FLjun may depend on the cytoplasmic N-tail binding first, followed by interactions with the luminal C-domain.

The data in Fig. 5 support our assumptions (a) that FLjun inserts into the bilayer, as do RyRs and variety of other membrane proteins, (b) after insertion, the short N-terminal domain is exposed to the cytoplasmic solution, while the highly charged C-terminus remains on the luminal side. The consistent increase in RyR activity after FLjun addition to the luminal solution suggests that FLjun routinely inserts into the bilayer in the same orientation.

**Regions in RyR1 that interact with junctin.** Cjun and Njun binding sites on RyR1 were examined using deletion mutations of rabbit RyR1 (Fig. 6A, Methods). Although RyR preparations were obtained from different species for reasons of availability and compatibility with affinity chromatography materials, the results appear to be largely species independent. It is notable that FLjun, Cjun and Njun bound to full length RyR1 from rabbit skeletal muscle, full length recombinant mouse RyR2 (Fig. 1C-F above), full length recombinant rabbit RyR1 (Fig. 6B&C and 7B&D below) and interacted consistently with full length RyR2 from sheep heart (Fig. 2 to 5 above).

RyR1 binding sites for Cjun. Cjun bound to RyR1 constructs **II** and **III**, containing RyR1 N-terminal residues 1-182 plus C-terminal residues 4008-4830, but did not bind substantially to cytoplasmic residues 1-182 alone (**VIII**), or 4254-4535 (**XII**) containing divergent region I (**D1**) (Fig. 6B&C). Cjun binding to construct **III** is significantly less than binding to **I** or **II**, indicating that residues 4831- 5837 containing the pore loop, influence Cjun binding to RyR1. However the major RyR1 binding sites for Cjun appear to be located between residues 4535-4830, containing the S1-S2 linker (as defined by (Ramachandran et al., 2013) and previously known as the M5-M6 linker (Zissimopoulos and Lai, 2007; Zorzato et al., 1990)), a region in human RyR2 that binds to junctin (Altschafli et al., 2011).

RyR1 binding sites for Njun. Njun bound to all RyR1 constructs containing residues 182-2156 (**I**, **IX**, **X** and **XI**, Fig. 7B and C), with little binding to the Njun<sub>scrambled</sub> peptide. Construct **XII** bound

similarly to Njun and Njun<sub>scrambled</sub> (Fig 7B), suggesting non-specific binding. None of **I**, **IX**, **X**, **XI** or **XII** bound to neutravidin agarose in the absence of peptide. However the 1-1078 construct (**XIII**) bound to neutravidin agarose and to Njun<sub>scrambled</sub> in greater amounts than Njun (Fig. 7B). Construct 1079-2156 (**XIV**) bound to Njun only, not to Njun<sub>scrambled</sub> or neutravidin agarose (Fig. 7B), indicating highly specific binding. To assess specific Njun binding, Njun<sub>scrambled</sub> densities for each construct were subtracted from Njun densities (Fig. 7C). The results indicate an N-terminal RyR1 binding site for Njun between residues 1097 and 2156 (**XIV**). Although Njun appears not to bind specifically to residues RyR1 1-1097 (**XIII**), a conclusion for this construct is complicated by its binding to streptavidin agarose.

**RyR binding residues in Cjun.** Cjun binds to the pore loop of RyR2 (Altschafli et al., 2011), a region of high charge density that, in RyR1, also binds to triadin (Goonasekera et al., 2007). A KEKE motif in triadin is implicated in binding to RyR1 (Wium et al., 2012) and we now explore RyR interactions with a similar KEKE-like motif in the C-terminal junctin residues 85-106 (Fig. 8A&B). The KEKE peptides (Fig. 8B), like Cjun, added to the luminal solution inhibited RyR channels with significant increases in closed times and decreases in open time (Fig. 8C-E). This contrasts with RyR1 activation produced by the triadin KEKE<sub>200-232</sub> peptide (Wium et al., 2012) which has a similar KEKE content (Fig. 8B). These opposite actions were not explored further, but may be due to the slightly different KEKE sequence in triadin and junctin, or to the extended hydrophobic C tail of the triadin peptide allowing additional RyR interactions. In contrast to Cjun, and similar to the triadin KEKE<sub>200-232</sub> peptide (Wium et al., 2012), the KEKE peptide in the cytoplasmic solution had no effect on RyR channels (Fig. 8C-E). In conclusion the KEKE motif in the junctin 84 to 106 region can bind to RyR1 and RyR2 and reproduce the effects of Cjun on the luminal side of the channels. Affinity chromatography reveals a strong association between the KEKE peptide and purified RyR1 or RyR2 (Fig. 8F&G).

## **DISCUSSION.**

We report a novel *in vitro* interaction between the N-terminal cytoplasmic residues of junctin and the cytoplasmic domains of RyR1 and RyR2, in addition to expected luminal interactions. We show that a binding site for the N-terminal domain of junctin resides in residues 1078-2156 of RyR1 and suggest that this cytoplasmic binding must be established before the luminal interaction in order to replicate the normal regulation of RyR channels by junctin. In addition to the cytoplasmic binding site, the results indicate that a RyR1 luminal binding site for junctin between residues 4535-4830 containing the S1-S2 linker that binds to junctin in human RyR2 (Altschafel et al., 2011). There is good sequence homology between rabbit RyR1 and RyR2 in the N- and C-terminal parts of this linker region, although the overall homology in residues 4535-4830 is only 75% (BLASTP 2.2.30+; Table S4). The very similar effects of junctin on RyR1 and RyR2 activity indicate that the functional binding is to regions conserved in the two RyR isoforms. Finally, this work reveals differences between the functional outcome of junctin and triadin interactions with RyRs, supporting the idea that two “anchoring” proteins have independent roles in Ca<sup>2+</sup> homeostasis. These differences include (a) several binding sites for junctin in contrast to a single triadin binding site in the RyR pore loop (Goonasekera et al., 2007), (2) RyR activation by the N-terminal domain of junctin, in contrast to inhibition by N-terminal triadin residues (Groh et al., 1999) and (3) the luminal KEKE rich region of junctin (aa86-107) inhibits RyRs, while the equivalent triadin region (aa200-232) activates RyR1 (Wium et al., 2012). These differences are consistent with reports that junctin communicates signals from CSQ1 to RyR1 (Wei et al., 2009a), while triadin influences EC coupling (Goonasekera et al., 2007).

**The significance of N-terminal junctin binding to RyRs.** The results suggest that the cytoplasmic site is physiological as it appears to be occupied by the endogenous junctin N-tail in the native channels. As noted above, we suggest that when FLjun is added to the luminal bilayer solution, its hydrophobic trans-membrane domain (residue 23-43) inserts into the bilayer such that the short N-terminus is located in the cytoplasmic solution and the C-terminal domain remains in the luminal solution (Wei et al., 2009a). Since the actions of luminal FLjun can only be replicated when Njun is added first to the cytoplasmic solution and then Cjun to the luminal solution, we suggests that FLjun insertion into the bilayer may allow the cytoplasmic interaction to anchor FLjun to the RyRs and facilitate the luminal interaction.

**Similar actions of junctin on RyR1 and RyR2.** It is notable that FLjun, Njun and Cjun bind similarly to cardiac and skeletal RyRs, with little RyR isoform-dependence in the functional effect of either cytoplasmic or luminal interactions. This is not surprising as the same junctin splice variant of

the aspartate- $\beta$ -hydroxylase gene is expressed in the heart and skeletal muscle. On the other hand there is considerable overall sequence diversity between RyR1 and RyR2, some regions of high homology exist. One explanation for the similar results is that the junctin binding sites are in regions of sequence homology in RyR1 and RyR2. Curiously, CSQ1 inhibits RyR1 by binding to junctin (Wei et al., 2009a), while CSQ2 activates RyR1 and RyR2 (Wei et al., 2009b). If RyR1/2 activation by CSQ2 is also through junctin, CSQ1 and CSQ2 must cause different conformational changes in junctin.

**Multiple junctin binding sites on RyRs.** The C-terminal domain of junctin binds to the S1-S2 (M5-M6) linker and the pore loop of RyR2 (Altschafel et al., 2011) and is likely to bind to the same regions in RyR1. We find that the residues including largely uncharged S1-S2 linker region of RyR1 bind to Cjun. The KEKE motif could well interact with charged residues in the pore loop as does the similar KEKE motif in triadin (Goonasekera et al., 2007; Wium et al., 2012). Both the cytoplasmic binding site and S1-S2 linker binding would help sustain full length junctin binding to mutant RyRs with acidic residues in the pore loop substituted with alanine (Goonasekera et al., 2007). KEKE motifs in junctin and triadin are implicated in binding not only to RyRs but also to CSQ. The same KEKE motif in triadin reportedly binds to both CSQ and the RyR, raising the possibility that both may not bind to triadin at the same time (Dulhunty et al., 2009). That triadin cannot convey signals from CSQ1 to RyR1 could be explained if CSQ1 binding to triadin disrupted triadin's association with RyR1 (Wei et al., 2009a). In contrast to triadin, junctin could convey signals from CSQ1 to RyR1 (Wei et al., 2009a), due to multiple RyR/junctin (this manuscript) and junctin/CSQ (Kobayashi et al., 2000) binding sites. Thus, junctin could remain anchored to RyR1, while also binding CSQ1 and allowing CSQ1 to influence RyR1 activity (Wei et al., 2009a).

There is a complex interaction between triadin, junctin, CSQ and RyRs in living cells. Our studies in myotubes (Goonasekera et al., 2007) and other studies in C2C12 cells (Wang et al., 2009) suggest that triadin is more involved in EC coupling, while junctin supports resting RyR activity and CSQ regulation of RyRs (Wei et al., 2009a). However junctin knockout, triadin knockout or triadin/junctin double knockout suggest that the triadin/CSQ complex has a greater impact on junctional structure than the junctin/CSQ complex (Boncompagni et al., 2012). It is likely that dynamic functional effects and long term structural effects reflect different aspects of  $\text{Ca}^{2+}$  homeostasis and that the transgenic results are complicated by changes in structure and in expression of CSQ and other junctional proteins.

**The physiological role of junctin.** It remains our hypothesis that junctin is involved in maintaining RyR activity at rest and in transmitting signals from CSQ to RyRs. This is a significant role given the deleterious effects of changes in resting RyR activity or "leak" in causing myopathies such as

central core disease and malignant hyperthermia in skeletal muscle (Dainese et al., 2009; Paolini et al., 2007) and in precipitating cardiac arrhythmia (Jiang et al., 2004; Terentyev et al., 2006). Indeed junctin knockout and knockout/mutation of CSQ both increase channel leak and lead to arrhythmia (Altschafli et al., 2011; Faggioni and Knollmann, 2012). In bilayer studies, experimental removal of CSQ2 from RyR2 increases the sensitivity of RyR2 to changes in luminal  $\text{Ca}^{2+}$ , in a manner that could lead to arrhythmia (Dulhunty et al., 2012). Similar changes in sensitivity to luminal  $[\text{Ca}^{2+}]$  are seen with junctin knockout (Altschafli et al., 2011) and are likely due to removal of the link to CSQ2.

**Conclusions.** The results reveal a strong interaction between the N-terminal tail of junctin and the cytoplasmic side of RyR1 channels and indicate that this interaction dictates the functional consequences of the full length protein binding to skeletal and cardiac RyR channels. A modulatory effect of the luminal C-terminal domain on the cytoplasmic N-terminal activation is essential to achieve the normal regulatory action of the full protein on channel activity. The multiple junctin binding sites on RyR1 and RyR2 raise the unexpected possibility that the influence of this anchoring protein on RyR activity is modified by factors in the cytoplasm as well as in the SR lumen.

## **METHODS**

**Materials**—DNA restriction and modifying enzymes, New England Biolabs and Roche Applied Science; T4 DNA ligase, Promega; Anti-green fluorescent protein (anti-GFP), Roche; anti-RyR (34C, anti-RyR DSHB), Developmental Studies Hybridoma Bank). Antibody against a junctin peptide (KLH-C-SKHTHSAKGNNQKRKN-OH; GL Biochem, Sanghai), IMVS Veterinary Services, Australia. PCR primers from GeneWorks, Australia.

**Species.** RyR1, RyR2 and junctin was sourced from several different species for various reasons including amounts required, compatibility with affinity chromatography materials and availability. Identity and homology between isoforms and species where known are given in Tables S1 to S4.

**FLjun (aa1-210) plasmids, expression and purification.** Full-length canine junctin in the pBlueScript II SK vector (Jones et al., 1995) was sub-cloned into a pET15b.ep (mod) vector using NdeI/BamHI sites.

Forward primer- 5′- GGG GGG CAT ATG GCT GAA GAG ACA AAG

Reverse primer- 5′- CGG GAT CCT CAG TTC TTC TTC TTC

The FLjun-pET15b.ep (mod) plasmid was transformed into *E. coli* BL21(DE3). Expression of the N-terminal His-tagged FLjun was induced by 0.6 mM isopropyl-β-D-thiogalactoside (IPTG) with 3-4 h incubation at 37°C. The cell pellet was resuspended in cold PBS (137 mM NaCl, 7 mM Na<sub>2</sub>HPO<sub>4</sub>, 2.56 mM NaH<sub>2</sub>PO<sub>4</sub>, pH 7.4) plus 1% Triton X-100, 5% glycerol and protease inhibitor cocktail tablet (Roche Diagnostics, Germany). The cells were lysed in 0.5 mg/ml lysozyme for 20 min on ice, sonicated and centrifuged twice at 15,000 x g for 25 min, then the supernatant centrifuged at 150,000 x g for 45 min. The final supernatant containing solubilised FLjun was incubated with Ni<sup>2+</sup>-nitrilotriacetic acid (NTA) agarose plus 25 mM imidazole at 4 °C for 2 h, the FLjun-poly His-Ni<sup>2+</sup>-NTA agarose complex washed in cold Buffer A (50 mM NaH<sub>2</sub>PO<sub>4</sub>, 300 mM NaCl, pH 8.0 with 1% Triton X-100, 5% glycerol and 25-35 mM imidazole) and the fusion protein eluted with Ni elution buffer (50 mM NaH<sub>2</sub>PO<sub>4</sub>, 300 mM NaCl, 250 mM imidazole, pH 8.0 with 1% Triton X-100 and 5% glycerol). The protein was concentrated and dialysed against MOPS buffer (20 mM MOPS, pH 7.4, 150 mM NaCl plus 0.2% Triton X-100 and 5% glycerol). Triton X-100 was removed by incubation with Bio-Beads SM-2 adsorbents (Bio-Rad) at room temperature for 1.75 h and the centrifugation (~1000 x g for 3 min). The supernatant containing purified FLjun was concentrated (centrifugal filter, Millipore) and stored -80 °C.

**Cjun (aa46-210) plasmids, expression and purification:** Cjun DNA was amplified from full length canine junctin in the pBlueScript II SK vector (Jones et al., 1995), cloned into pGADT7 vector and sub-cloned from pGADT7-CJun into the pET15b.ep vector using NdeI/BamHI sites.

Forward primer 5'-CGGAAT TCCTTGTTGAT TATGAAGAAG TT

Reverse primer 5'-CGGGATCCTCAGTTCTTCCTC TCTGG T

Cjun was also expressed in pHUE (Baker et al., 2005; Catanzariti et al., 2004) for poly His removal, and obtained from Cjun- pET15b.ep:

forward primer 5'- GACCCGCGGTGGACTTGTTGATTATGAAG

reverse primers 5'- CGAAGCTT TCAGTTCTTCCTCTTC

The Cjun-pET15b.ep plasmid was transformed into *E. coli* BL21/DE3. Expression of the N terminal His-tagged protein was induced by 0.6 mM isopropyl-β-D-thiogalactoside (IPTG). Cjun was purified from the soluble lysate fraction using Buffer A (50 mM phosphate buffer PH 8 and 300 mM NaCl) with Ni-agarose affinity chromatography. The solution was exchanged for 20 mM MOPS, pH 7.4 and 150 mM NaCl, then Cjun concentrated (centrifugal filter, Millipore) and stored at -80° C.

Cjun-pHUE was also transformed and poly His-ubiquitin tagged Cjun expressed in *E. coli* BL21DE3 (as Cjun-pET15b.ep). The poly His-ubiquitin tag was removed (Baker et al., 2005; Catanzariti et al., 2004) and Cjun purified, concentrated and stored at -80° C.

**RyR1 plasmids, expression and isolation.** Numerals in parentheses refer to constructs defined in Fig. 6A&7A. **GFL (I)** (RyR1 5'EGFP tagged), **Gbhat (II)** (aa 1-182/4008-End) and **SM1 (III)** (aa1-182/4008-4830) are described previously (Bhat et al., 1997; Treves et al., 2002; Zorzato et al., 1990). **SM2 (VIII)** (aa1-182): SallI546/SallI<sub>polylinker</sub> removed from GFL and the remaining GFL re-ligated. **(IX)**, aa1-3724; **(X)**, aa1-2746; **(XI)**, aa1-2156; **(XII)**, RyR1 aa4254-4535; **(XIII)**, aa1-1078; and **(XIV)**, aa1079-2156 plasmids in pJ204, from DNA2.0 (Menlo Park, CA), were digested by HindIII and KpnI and cloned in frame into the HindIII and KpnI sites in pEGFP-C3 vector polylinker. RyR1 constructs were expressed in HEK293 cells and protein isolated (Goonasekera et al., 2007). Microsomal vesicles were prepared and stored at -80° C. Mouse RyR2, stably expressed in an inducible HEK293 cell line (Koop et al., 2008), was isolated with the same method as RyR1.

All FLjun, Cjun and RyR constructs were sequenced by the JCSMR Biomolecular Resource Facility.

**Peptide Synthesis** - The following peptides were synthesised by the JCSMR BRF, with purification using HPLC and mass spectroscopy.

Njun: <sup>1</sup>MAEETKHGGHKNRKGGLSQSS<sup>22</sup>

Njun<sub>scrambled</sub>: STGENKGHGLSGKHKSEGRAMG

Cjun<sub>KEKEcanine</sub> <sup>84</sup>KRKTKAKVKELTKEELKKEKEK<sup>105</sup>

Cjun<sub>KEKErabbit</sub> <sup>53</sup>KRKTKAKVKELIKEELKKGKEK<sup>74</sup>

Peptides for affinity chromatography were constructed with N-terminal biotin tag. Rabbit KEKE motif peptides were tested because RyR1 and some FLjun were isolated from rabbit muscle. The

canine KEKE motif was also tested because recombinant canine FLjun was also used (see Isolation of FLjun below) and Cjun was derived from canine cardiac junctin. Note that the KEKE sequence is identical in canine junctin (Fig. 8) and human junctin used by (Altschafel et al., 2011).

**SR vesicle isolation, RyR purification.** Rabbit skeletal SR and sheep ventricular SR vesicles were isolated and RyRs purified (Wei et al., 2009b). Sucrose gradient fractions containing RyRs (Western blot detection) were concentrated, 15  $\mu$ l aliquots frozen and stored at  $-80^{\circ}$  C.

**Co-immunoprecipitation.** Co-IP was used to assess Cjun binding to native or recombinant RyRs and RyR1 constructs (Beard et al., 2008; Wei et al., 2006). 100  $\mu$ g of purified RyRs or 3  $\mu$ g of Cjun were diluted to 100  $\mu$ l in IP buffer (0.025 M Tris, 0.15 M NaCl, 0.001 M EDTA, 1% NP-40, 5% glycerol, pH 7.4) and pre-cleared by rotation for 2 h at  $4^{\circ}$  C with 100  $\mu$ l of washed control agarose resin. 1  $\mu$ l of anti-junctin was diluted to 100  $\mu$ l in coupling buffer (0.01 M sodium phosphate, 0.15 M NaCl, pH 7.2), rotated with 25  $\mu$ l of washed and equilibrated protein A/G agarose for 2 h at room temperature with addition of 3  $\mu$ l sodium cyanoborohydride, then washed, quenched, and re-equilibrated with IP buffer. The antibody/agarose was then incubated overnight at  $4^{\circ}$  C with either 3  $\mu$ g of the pre-cleared Cjun or with IP buffer alone, then incubated with 100  $\mu$ g of pre-cleared RyR or RyR1 constructs for 2 h at room temperature. Each incubation was followed by 3-4 wash and centrifugation steps. In the reverse assay, 1  $\mu$ l of  $^{34}$ C anti-RyR1/2 or anti-GFP was diluted to 100  $\mu$ l in coupling buffer, bound to protein A/G agarose, coupled with 10  $\mu$ g of pre-cleared RyRs or RyR1 constructs, then incubated with 10  $\mu$ g of pre-cleared Cjun. Proteins were eluted by boiling for 5 min in 15-20  $\mu$ l of Laemmli sample buffer and 5 to 10  $\mu$ l loaded onto SDS-PAGE gels. Importantly, a constant volume was added for each series of experiments. Proteins were separated on SDS-PAGE, transferred to PVDF (polyvinyl difluoride) membrane and immunoprobed with  $^{34}$ C anti-RyR1/2 or anti-GFP to detect RyR, or with anti-junctin to detect Cjun.

**NeutrAvidin agarose affinity chromatography.** Binding of Njun and Njun<sub>scrambled</sub> to native or recombinant RyRs or RyR1 fragments was detected by affinity chromatography (Rebbeck et al., 2011; Wium et al., 2012). 100  $\mu$ l of NeutrAvidin agarose (Thermoscientific, Rockford, IL) was washed twice in wash buffer (PBS + 0.1% SDS) and then resuspended to 100  $\mu$ l in the same buffer. 100  $\mu$ g of biotinylated peptide was diluted to 1  $\mu$ g/ $\mu$ l in binding/wash buffer (PBS + 0.1% SDS), added to 100  $\mu$ l of agarose slurry, incubated for 2.5 h at room temperature, and then washed 5 times with centrifugation (1000 x g for 3 min) in wash buffer. Purified RyR protein (90  $\mu$ g) was diluted in wash buffer plus protease inhibitor (AEBSF (Sigma-Aldrich, USA) or Complete EDTA-free protease Inhibitor Cocktail (Roche Diagnostics, Germany)), precleared with control agarose resin (200  $\mu$ l) for 2 h at room temperature, incubated with NeutrAvidin-agarose-bound biotinylated peptide or NeutrAvidin-agarose alone overnight at  $4^{\circ}$ C, then washed 5 times as above. Protein was eluted at

65°C for 10 min in 15-20 ul of Laemmli sample buffer and 5 to 10 ul loaded onto SDS-PAGE gels. Importantly, a constant volume was added for each series of experiments. Proteins were separated on SDS-PAGE, transferred to PVDF membrane and immunoprobed with 34C anti-RyR1/2 or anti-GFP to detect RyR protein, or with StrepTactin to detect biotinylated peptides.

**Isolation of FLjun.** Junctin was isolated from rabbit skeletal junctional face membrane (JFM) using SDS preparative gel electrophoresis in a Bio-Rad 491 prep cell (Wei et al., 2009a). JFM was solubilized in 1%/0.5% CHAPS/PC, 1 mM DTT, 1 M NaCl, 20 mM MOPS, and 200  $\mu$ M EGTA pH 7.4 with protease inhibitors, on ice for 1h, then centrifuged at 135,000  $\times$ g for 15 min. The supernatant was diluted with sample buffer (188 mM Tris-HCl, pH 6.8, 30% glycerol, 6% SDS, 0.06% bromophenol blue, and 15%  $\beta$ -mercaptoethanol), and boiled for 5 min before loading onto a 6.5 cm vertical cylindrical polyacrylamide gel. The resolving gel contained 12% acylamide/bis (37.5:1), 0.375 M Tris-HCl (pH 8.8), 0.025% ammonium persulphate (APS), and 0.025% *N,N,N,N*-Tetramethylethylenediamine (TEMED). A stacking gel, double the sample volume, contained 4% acylamide/bis (37.5:1), 0.125 M Tris-HCl (pH 6.8), 0.05% (APS), and 0.1% TEMED. Electrophoresis was at 40 mA in 25 mM Tris, 191mM glycine, 0.1% SDS, pH 8.3. Eighty 2 ml fractions were collected at a flow of 1ml/min and analysed by SDS-PAGE and immunoblot. Junctin was renatured after precipitation in 400 mM KCl for 20 min at room temperature with gentle agitation. The fractions were centrifuged ( $\sim$ 15,800  $\times$  g) for 15 min, the protein eluted and re-folded by detergent exchange in 0.2% Triton X-100, 20 mM MOPS, 150 mM KCl, 200  $\mu$ M EGTA, pH 7.4 plus protease inhibitors, at room temperature for 1 h, then centrifuged ( $\sim$ 15,800  $\times$  g) for 10 min to remove SDS-KCl precipitate. The supernatant protein was concentrated and exchanged with 20 mM MOPS pH 7.4, 150 mM NaCl, 200 $\mu$ M EGTA + protease inhibitors) using Millipore Amicon Ultra-4 centrifugal filters. Purified junctin (0.2-0.4 mg/ml) was stored at -70°C.

NB, FLjun isolated from rabbit skeletal muscle was initially used in binding and bilayer experiments. However the extraction was lengthy and yields were very low and we obtained better yields with recombinant canine junctin. There was no observable difference between results obtained with the recombinant FLjun and FLjun isolated from skeletal muscle and both was combined in average data.

**Single channel recording and analysis.** RyRs were incorporated into lipid bilayers and channel activity recorded using standard techniques (Beard et al., 2008; Wium et al., 2012). *Cis* (cytoplasmic)  $\text{Ca}^{2+}$  was adjusted to 1  $\mu$ M or 100 nM with [BAPTA] determined using a  $\text{Ca}^{2+}$  electrode. *Trans* [ $\text{Ca}^{2+}$ ] was 1 mM throughout. Open probability ( $P_o$ ), mean open ( $T_o$ ), mean closed ( $T_c$ ), time or fractional mean current ( $I'_F$ ) were measured (Beard et al., 2008; Wei et al., 2006). Open

and closed time constants, determined using logged bin analysis (Sigworth and Sine, 1987; Tae et al., 2011), were assigned to  $\tau_{O1}$  or  $\tau_{C1}$  (1-10 ms),  $\tau_{O2}$  or  $\tau_{C2}$  (10-50 ms) or to  $\tau_{O3}$  or  $\tau_{C3}$  (50-500 ms).

**Ca<sup>2+</sup> release from SR vesicles.** Extravesicular Ca<sup>2+</sup> was measured spectrophotometrically at 710 nm, using the Ca<sup>2+</sup> indicator antipyrylazo III was determined following Ca<sup>2+</sup> loading and block of the Ca<sup>2+</sup> pump with thapsigargin (Hanna et al., 2011; Jalilian et al., 2008).

**Statistics.** Data are presented as mean  $\pm$ SEM and significance evaluated using paired or unpaired Student's t-test or ANOVA as appropriate. The number of observations (n) are given. As similar results were obtained at +40 mV and -40 mV in bilayer experiments, data for each potential was normally included in average data, i.e. 2 observations for each channel under each condition. To reduce effects of normal variability in the control parameters for RyRs, data with junctin constructs (P<sub>o</sub>J, T<sub>o</sub>J, T<sub>c</sub>J) are expressed relative to control (P<sub>o</sub>C, T<sub>o</sub>C, T<sub>c</sub>C), (eg  $\log P_{oJ} - \log P_{oC}$ ).

## ACKNOWLEDGEMENTS

We thank Ms Joan Stivala for assistance with SR vesicle isolation and Ms Umayal Narayanan for assistance with protein expression and isolation. The work was supported by Australian Research Council grants (DP1094219 and DP130100592 to AFD and NAB) and National Health and Medical Research Council Project grant APP585474 to AFD and NAB, and a NHMRC Career Development Award APP1003985 to NAB.

## REFERENCES.

- Altschafli, B. A., Arvanitis, D. A., Fuentes, O., Yuan, Q., Kranias, E. G. and Valdivia, H. H. (2011). Dual role of junctin in the regulation of ryanodine receptors and calcium release in cardiac ventricular myocytes. *J Physiol.* 589, 6063-80.
- Baker, R. T., Catanzariti, A. M., Karunasekara, Y., Soboleva, T. A., Sharwood, R., Whitney, S. and Board, P. G. (2005). Using deubiquitylating enzymes as research tools. *Methods Enzymol.* 398, 540-54.
- Beard, N. A., Sakowska, M. M., Dulhunty, A. F. and Laver, D. R. (2002). Calsequestrin is an inhibitor of skeletal muscle ryanodine receptor calcium release channels. *Biophys J.* 82, 310-20.
- Beard, N. A., Wei, L., Cheung, S. N., Kimura, T., Varsanyi, M. and Dulhunty, A. F. (2008). Phosphorylation of skeletal muscle calsequestrin enhances its Ca<sup>2+</sup> binding capacity and promotes its association with junctin. *Cell calcium.* 44, 363-73.
- Bhat, M. B., Zhao, J., Zang, W., Balke, C. W., Takeshima, H., Wier, W. G. and Ma, J. (1997). Caffeine-induced release of intracellular Ca<sup>2+</sup> from Chinese hamster ovary cells expressing skeletal muscle ryanodine receptor. Effects on full-length and carboxyl-terminal portion of Ca<sup>2+</sup> release channels. *J Gen Physiol.* 110, 749-62.
- Boncompagni, S., Thomas, M., Lopez, J. R., Allen, P. D., Yuan, Q., Kranias, E. G., Franzini-Armstrong, C. and Perez, C. F. (2012). Triadin/Junctin double null mouse reveals a differential role for Triadin and Junctin in anchoring CASQ to the jSR and regulating Ca<sup>2+</sup> homeostasis. *PLoS One.* 7, e39962.
- Catanzariti, A. M., Soboleva, T. A., Jans, D. A., Board, P. G. and Baker, R. T. (2004). An efficient system for high-level expression and easy purification of authentic recombinant proteins. *Protein science : a publication of the Protein Society.* 13, 1331-9.
- Dainese, M., Quarta, M., Lyfenko, A. D., Paolini, C., Canato, M., Reggiani, C., Dirksen, R. T. and Protasi, F. (2009). Anesthetic- and heat-induced sudden death in calsequestrin-1-knockout mice. *FASEB J.* 23, 1710-20.
- Dulhunty, A., Wei, L. and Beard, N. (2009). Junctin - the quiet achiever. *J Physiol.* 587, 3135-7.
- Dulhunty, A. F., Laver, D. R., Gallant, E. M., Casarotto, M. G., Pace, S. M. and Curtis, S. (1999). Activation and inhibition of skeletal RyR channels by a part of the skeletal DHPR II-III loop: effects of DHPR Ser687 and FKBP12. *Biophys J.* 77, 189-203.
- Dulhunty, A. F., Wium, E., Li, L., Hanna, A. D., Mirza, S., Talukder, S., Ghazali, N. A. and Beard, N. A. (2012). Proteins within the intracellular calcium store determine cardiac RyR channel activity and cardiac output. *Clin Exp Pharmacol Physiol.* 39, 477-84.

- Faggioni, M. and Knollmann, B. C. (2012). Calsequestrin 2 and arrhythmias. *Am J Physiol Heart Circ Physiol.* 302, H1250-60.
- Goonasekera, S. A., Beard, N. A., Groom, L., Kimura, T., Lyfenko, A. D., Rosenfeld, A., Marty, I., Dulhunty, A. F. and Dirksen, R. T. (2007). Triadin binding to the C-terminal luminal loop of the ryanodine receptor is important for skeletal muscle excitation contraction coupling. *J Gen Physiol.* 130, 365-78.
- Groh, S., Marty, I., Ottolia, M., Prestipino, G., Chapel, A., Villaz, M. and Ronjat, M. (1999). Functional interaction of the cytoplasmic domain of triadin with the skeletal ryanodine receptor. *J Biol Chem.* 274, 12278-83.
- Gyorke, S. and Carnes, C. (2008). Dysregulated sarcoplasmic reticulum calcium release: potential pharmacological target in cardiac disease. *Pharmacol Ther.* 119, 340-54.
- Hanna, A. D., Janczura, M., Cho, E., Dulhunty, A. F. and Beard, N. A. (2011). Multiple actions of the anthracycline daunorubicin on cardiac ryanodine receptors. *Mol Pharmacol.* 80, 538-49.
- Jalilian, C., Gallant, E. M., Board, P. G. and Dulhunty, A. F. (2008). Redox potential and the response of cardiac ryanodine receptors to CLIC-2, a member of the glutathione S-transferase structural family. *Antioxid Redox Signal.* 10, 1675-86.
- Jiang, D., Xiao, B., Yang, D., Wang, R., Choi, P., Zhang, L., Cheng, H. and Chen, S. R. (2004). RyR2 mutations linked to ventricular tachycardia and sudden death reduce the threshold for store-overload-induced  $Ca^{2+}$  release (SOICR). *Proc Natl Acad Sci U S A.* 101, 13062-7.
- Jones, L. R., Zhang, L., Sanborn, K., Jorgensen, A. O. and Kelley, J. (1995). Purification, primary structure, and immunological characterization of the 26-kDa calsequestrin binding protein (junctin) from cardiac junctional sarcoplasmic reticulum. *J Biol Chem.* 270, 30787-96.
- Kobayashi, Y. M., Alseikhan, B. A. and Jones, L. R. (2000). Localization and characterization of the calsequestrin-binding domain of triadin 1. Evidence for a charged beta-strand in mediating the protein-protein interaction. *J Biol Chem.* 275, 17639-46.
- Koop, A., Goldmann, P., Chen, S. R., Thieleczek, R. and Varsanyi, M. (2008). ARVC-related mutations in divergent region 3 alter functional properties of the cardiac ryanodine receptor. *Biophys J.* 94, 4668-77.
- Laver, D. R. (2005). Coupled calcium release channels and their regulation by luminal and cytosolic ions. *Eur Biophys J.* 34, 359-68.
- Laver, D. R., Roden, L. D., Ahern, G. P., Eager, K. R., Junankar, P. R. and Dulhunty, A. F. (1995). Cytoplasmic  $Ca^{2+}$  inhibits the ryanodine receptor from cardiac muscle. *J Membr Biol.* 147, 7-22.
- Oddoux, S., Brocard, J., Schweitzer, A., Szentesi, P., Giannesini, B., Faure, J., Pernet-Gallay, K., Bendahan, D., Lunardi, J., Csernoch, L. et al. (2009). Triadin deletion induces impaired skeletal muscle function. *J Biol Chem.* 284, 34918-29.

- Pagala, M. K. and Taylor, S. R. (1998). Imaging caffeine-induced  $\text{Ca}^{2+}$  transients in individual fast-twitch and slow-twitch rat skeletal muscle fibers. *The American journal of physiology*. 274, C623-32.
- Paolini, C., Quarta, M., Nori, A., Boncompagni, S., Canato, M., Volpe, P., Allen, P. D., Reggiani, C. and Protasi, F. (2007). Reorganized stores and impaired calcium handling in skeletal muscle of mice lacking calsequestrin-1. *J Physiol*. 583, 767-84.
- Ramachandran, S., Chakraborty, A., Xu, L., Mei, Y., Samsó, M., Dokholyan, N. V. and Meissner, G. (2013). Structural determinants of skeletal muscle ryanodine receptor gating. *The Journal of biological chemistry*. 288, 6154-65.
- Rebbeck, R. T., Karunasekara, Y., Gallant, E. M., Board, P. G., Beard, N. A., Casarotto, M. G. and Dulhunty, A. F. (2011). The beta(1a) subunit of the skeletal DHPR binds to skeletal RyR1 and activates the channel via its 35-residue C-terminal tail. *Biophys J*. 100, 922-30.
- Saito, A., Seiler, S., Chu, A. and Fleischer, S. (1984). Preparation and morphology of sarcoplasmic reticulum terminal cisternae from rabbit skeletal muscle. *J Cell Biol*. 99, 875-85.
- Sigworth, F. J. and Sine, S. M. (1987). Data transformations for improved display and fitting of single-channel dwell time histograms. *Biophys J*. 52, 1047-54.
- Tae, H. S., Cui, Y., Karunasekara, Y., Board, P. G., Dulhunty, A. F. and Casarotto, M. G. (2011). Cyclization of the intrinsically disordered alpha1S dihydropyridine receptor II-III loop enhances secondary structure and in vitro function. *J Biol Chem*. 286, 22589-99.
- Terentyev, D., Nori, A., Santoro, M., Viatchenko-Karpinski, S., Kubalova, Z., Gyorke, I., Terentyeva, R., Vedamoorthyrao, S., Blom, N. A., Valle, G. et al. (2006). Abnormal interactions of calsequestrin with the ryanodine receptor calcium release channel complex linked to exercise-induced sudden cardiac death. *Circ Res*. 98, 1151-8.
- Tinker, A. and Williams, A. J. (1993). Probing the structure of the conduction pathway of the sheep cardiac sarcoplasmic reticulum calcium-release channel with permeant and impermeant organic cations. *J Gen Physiol*. 102, 1107-29.
- Treves, S., Pouliquin, R., Moccagatta, L. and Zorzato, F. (2002). Functional properties of EGFP-tagged skeletal muscle calcium-release channel (ryanodine receptor) expressed in COS-7 cells: sensitivity to caffeine and 4-chloro-m-cresol. *Cell calcium*. 31, 1-12.
- Wang, Y., Li, X., Duan, H., Fulton, T. R., Eu, J. P. and Meissner, G. (2009). Altered stored calcium release in skeletal myotubes deficient of triadin and junctin. *Cell calcium*. 45, 29-37.
- Wei, L., Gallant, E. M., Dulhunty, A. F. and Beard, N. A. (2009a). Junctin and triadin each activate skeletal ryanodine receptors but junctin alone mediates functional interactions with calsequestrin. *Int J Biochem Cell Biol*. 41, 2214-24.

- Wei, L., Hanna, A. D., Beard, N. A. and Dulhunty, A. F. (2009b). Unique isoform-specific properties of calsequestrin in the heart and skeletal muscle. *Cell Calcium*. 45, 474-84.
- Wei, L., Varsanyi, M., Dulhunty, A. F. and Beard, N. A. (2006). The conformation of calsequestrin determines its ability to regulate skeletal ryanodine receptors. *Biophys J*. 91, 1288-301.
- Wium, E., Dulhunty, A. F. and Beard, N. A. (2012). A skeletal muscle ryanodine receptor interaction domain in triadin. *PloS One*. 7, e43817.
- Zissimopoulos, S. and Lai, F. A. (2007). Ryanodine receptor structure, function and pathophysiology. . In: Krebs J, Michalak M, editors. *Calcium: A Matter of Life or Death*:. Elsevier B.V., 227-342.
- Zorzato, F., Fujii, J., Otsu, K., Phillips, M., Green, N. M., Lai, F. A., Meissner, G. and MacLennan, D. H. (1990). Molecular cloning of cDNA encoding human and rabbit forms of the Ca<sup>2+</sup> release channel (ryanodine receptor) of skeletal muscle sarcoplasmic reticulum. *J Biol Chem*. 265, 2244-56.

## FIGURE LEGENDS.

**Fig. 1. Junctin structure and binding to RyRs.** **A)** Junctin topology showing the cytoplasmic N-terminal domain, the transmembrane and C-terminal domains. **B)** Purification of FLjun and recombinant Cjun. Upper, coomassie stain (SDS-PAGE) shows FLjun (lane 1), 6-his Cjun (lane 2) and Cjun after his-tag removal (lane 3). Lower, Western Blot (anti-junctin antibody). **C)** Co-IP of RyR1 by FLjun and 6-his Cjun, or RyR2 by FLjun and by 6-his Cjun (lanes 1 to 4). No RyR1 or RyR2 bound to the beads or the anti-junctin antibody in the absence of FLjun or Cjun (lanes 5 and 6). **D)** Average densitometry of RyR/FLjun or RyR/Cjun (RyR2, n=5; RyR1, n=4). Asterisks (\*) indicate RyR2 values significantly less than RyR1. P values below bins are for differences between **(a)** FLjun and Cjun bound to RyR2 or RyR1, and **(b)** FLjun bound to RyR1 and FLjun bound to RyR2, or Cjun bound to RyR1 and Cjun bound to RyR2. **E)** Co-IP of RyR2 and RyR1 by biotinylated Njun or biotinylated scrambled Njun peptide (Njun<sub>sc</sub>). **F)** Average RyR/Njun or RyR/Njun<sub>sc</sub> (RyR2, n=7; RyR1, n=8). Asterisks (\*) indicate RyR/Njun<sub>sc</sub> values significantly less than RyR/Njun. P values below bins **(a)** are for differences between Njun and Njun<sub>scrambled</sub> binding to RyR2 or RyR1

**Fig. 2. Activation of purified RyR2 and RyR1 channels by luminal FLjun.** **A** and **B)** 3 s of purified RyR activity at -40 mV. Channel opening is downward, from zero current (continuous line, c) to maximum single channel conductance (broken line, o), here and in Figs. 3, 4, 5 and 8 below. The upper trace in each panel shows control activity and the lower trace after adding 213 nM (5 µg/ml) FLjun to the luminal solution bathing RyR2 (**A**) or RyR1 (**B**). **C-E)** average of relative open probability ( $\log P_{oJ} - \log P_{oC}$ ), mean open time ( $\log T_{oJ} - \log T_{oC}$ ) and mean closed time ( $\log T_{cJ} - \log T_{cC}$ ), determined for individual RyR2 (n=14) and RyR1 (n=10) channels. **F** and **G)** Effects of FLjun on average open (left) and closed (right) time constants and fraction of events in each time constant (Sigworth and Sine, 1987). The probability of events falling into each time constant is plotted against the time constant (in ms), for control data (open circles) and with FLjun (filled circles) for RyR2 (**F**) or RyR1 (**G**). Here and in Figures 3, 4, 5 and 8, (a) horizontal and vertical bars indicate the SEMs for time constant and probability respectively and are contained within the symbols if not visible and (b) p values below bins test are for differences between the probability of events (**p**, upper row) or time constant ( $\tau$ , lower row) with FLjun and control. Asterisks (\*) indicate significant differences between control and FLjun data. **H)** shows average open probability of native RyR2 (n=8) and RyR1 channels (n=12) exposed to FLjun, relative to open probability prior to exposure. P values below the bins in **C-E** and in **H** are for differences between FLjun and control parameters.

**Fig. 3. Cytoplasmic Njun activates purified RyR2 and RyR1 channels.** **A and B)** Records of 3 s of purified RyR channel activity at  $-40$  mV. The upper trace in each panel shows control activity and the lower trace activity in the same channel after adding cytoplasmic 213 nM Njun to RyR2 (**A**) and RyR1 (**B**). **C-E)** Average  $\log P_o J - \log P_o C$ ,  $\log T_o J - \log T_o C$  and  $\log T_c J - \log T_c C$ , defined in the legend to Fig. 2, for RyR2 (n=14) and RyR1 (n=10). **F)** 213 nM Njun<sub>scrambled</sub> added to the cytoplasmic solution, RyR2 (n=8) or RyR1 (n=16). **G and H)** Effects of 213 nM Njun on average open (left) and closed (right) time constants. The probability of events falling into each time constant is shown for control (open circles) and with 213 nM Njun (filled circles) for RyR2 (**G**) or RyR1 (**H**). Further details, including definition of p values above the x axis are described in the legend to Fig. 2. **I)** 213 nM Njun to the luminal solution, RyR2 (n=8) or RyR1 (n=14). **J-L)** 213 nM Njun to the cytoplasmic side of native RyRs - average  $\log P_o J - \log P_o C$ ,  $\log T_o J - \log T_o C$  and  $\log T_c J - \log T_c C$ , for RyR2 (n=13) and RyR1 (n=14). **M)** - The rate of  $Ca^{2+}$  release from  $Ca^{2+}$ -loaded SR vesicles after blocking SERCA with thapsigargin. Immediate effect of Njun on cardiac SR (n=4), and skeletal SR (n=4). Effect of preincubation with 5  $\mu$ M Njun on caffeine induced  $Ca^{2+}$  release through RyR2 (5 mM caffeine, n=7) and RyR1 (0.5 mM caffeine, n=11). Asterisks (\*) in all graphs indicate significant differences between control and junctin construct data. In **C-F, I-L and M**, p values for differences between Njun or Njun<sub>scrambled</sub> and control are given below the bins.

**Fig. 4. Cjun inhibits native RyR2 and RyR1 channels.** **A and B)** The upper trace in each panel shows control activity and the lower trace activity after adding 213 nM Cjun to the luminal solution, 3 s at  $-40$  mV. **C-E)** average  $\log P_o J - \log P_o C$ ,  $\log T_o J - \log T_o C$  and  $\log T_c J - \log T_c C$ , as defined in the legend to Fig. 2, for luminal addition of Cjun to purified RyR2 (n=18) and RyR1 (n=16) (black bins); cytoplasmic Cjun on purified RyR2 (n=32) and RyR1 (n=12) (cross-hatched bins); cytoplasmic Cjun on native RyR2 (n=8) and RyR1 (n=6) (hatched bin); cytoplasmic recombinant FLjun on purified RyR2 (n=12) and RyR1 (n=14) (grey bin). **F and G)** Effects of luminal 213 nM Cjun on average open (left) and closed (right) time constants as described for Figs. 2 and 3. Asterisks (\*) indicate significant differences between the fraction of events in a particular time constant group under control conditions and with 213 nM Cjun. **H)** Effect of luminal 213 nM boiled Cjun on relative open probability of RyR2 (n=5) and RyR1 (n=10). **I)** Effect of 5 $\mu$ M Cjun on the relative rate of  $Ca^{2+}$  release from SR vesicles immediately after application (left: cardiac n=5; skeletal n=5) and on caffeine induced  $Ca^{2+}$  release after 20 min pre-incubation and 10 min exposure during  $Ca^{2+}$  loading (right, cardiac n=5; skeletal n=5). P values for differences between rates with Cjun and buffer are given below the bins. **J)** Western blots probed for RyR, skeletal triadin (Trisk95), CSQ, triadin 2 and junctin. From left to right: cardiac SR (SR<sub>C</sub>); purified RyR2; skeletal SR (SR<sub>sk</sub>); purified RyR1. **K-L)** Average densitometry data from Western Blots of SR and purified RyR from cardiac (n=4) and

skeletal (n=4) muscle. Average RyR/junctin; p value for the difference between cardiac and skeletal SR is give below the bin (**K**). Junctin/RyR ratios show no significant junctin density in the purified preparations: p values for differences between SR and purified RyR are given below the bins; # indicates significantly lower ratio reflecting less junctin (**L**).

**Fig. 5. Channel activity after adding Njun to the cytoplasmic solution, then Cjun to the luminal solutions, reproduces activity seen after adding FLjun to the luminal solution. A-F)**

Data from 3 different experiments is compared in each graph. First, 213 nM FLjun added alone to the luminal solution (stippled bins - data from Fig. 2, included for comparison). Second, addition of 213nM Njun cytoplasmically, then 213 nM Cjun to the luminal solution (black bins: RyR2, n=10; RyR1, n=10). Third, addition of 213 nM Cjun luminally, then 213 nM Njun to the cytoplasmic solution (grey bins: RyR2, n=8; RyR1, n=10). **A and D**)  $\log P_{oJ} - \log P_{oC}$ ; **B and E**)  $\log T_{oJ} - \log T_{oC}$ ; **C and F**)  $\log T_{cJ} - \log T_{cC}$ , as defined in the legend to Fig. 2. (\*): significant difference between control parameters and with 213 nM FLjun, Cjun or Njun, p values beneath in row (a). (@): significant difference between parameters with luminal FLjun and with cytoplasmic Njun or luminal Cjun, p values beneath in row (b). (#): significant effect of adding luminal Cjun after cytoplasmic Njun (2<sup>nd</sup> black bin), or adding cytoplasmic Njun after luminal Cjun (2<sup>nd</sup> grey bin), p values beneath in row (c). The red dots indicate changes in open probability and mean closed time that are not significantly different (p values in red font) with luminal addition of FLjun alone or with luminal Cjun added after cytoplasmic Njun.

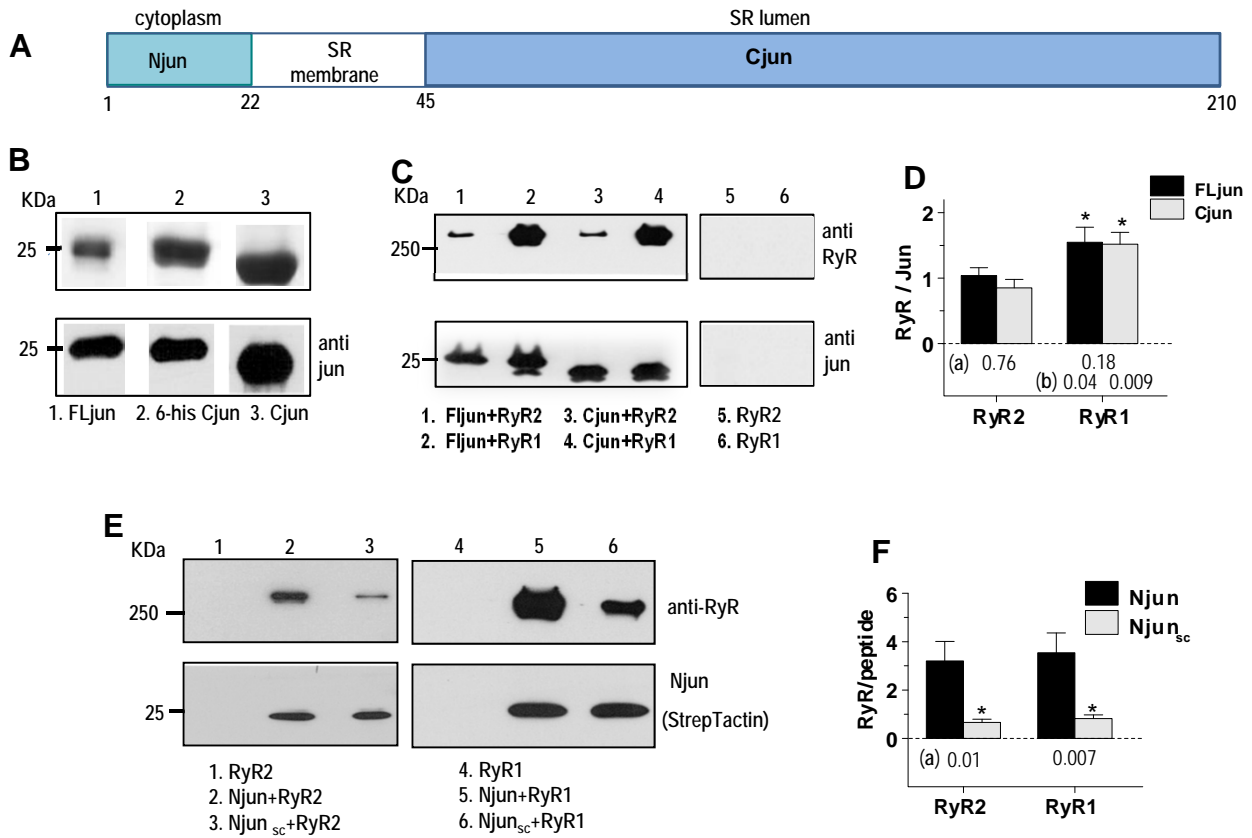
**Fig. 6. Regions of RyR1 that interact with Cjun. A)** Fragments of RyR1 examined for Cjun binding. Boxes indicate recombinant fragments. **B)** Co-IP of recombinant RyR1 and RyR1 fragments by Cjun bound to the anti-junctin antibody/protein A/G agarose. RyR fragments identified by anti GFP antibody, Cjun identified by anti-junctin antibody. **C)** Average density of RyR1 constructs, relative to the density of Cjun in the same lane as shown in **B** (n=3-5). (\*) shows significant differences between WT RyR1 and indicated fragment, p values are given beneath bins.

**Fig. 7. Regions of RyR1 that interact with Njun. A)** Fragments of RyR1 (boxes) examined for Njun binding. **B)** Affinity chromatography of RyR1 or RyR1 fragments bound to biotinylated Njun or Njun<sub>scrambled</sub> peptide associated with streptavidin agarose. RyR fragments identified by anti-GFP antibody, biotinylated peptides detected by StrepTactin-HRP conjugate. The RyR constructs are listed in the upper row above each lane, and the peptide (second row: Njun (Nj) or Njun<sub>scrambled</sub> (sc)). Three lanes are shown for RyR1 **XIII** and **XIV**, the first the result of adding **XIII** and **XIV** to streptavidin agarose in the absence biotinylated peptide, showing non-specific binding of **XIII**, but not **XIV** to beads. **C)** Average density of each RyR1 band relative to the density of Njun

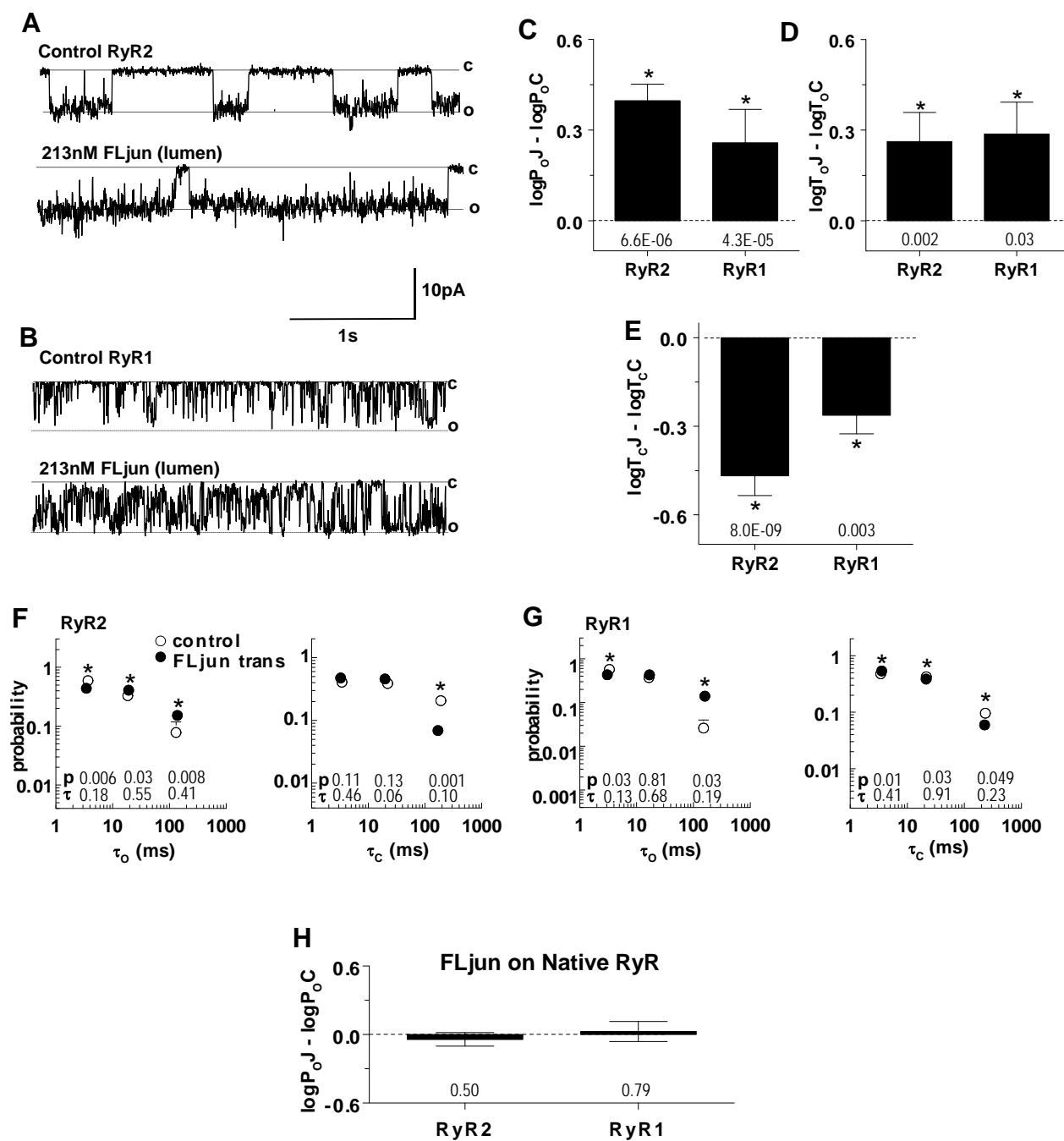
(RyR1/Njun) minus RyR1 density relative to Njun<sub>scrambled</sub> (RyR1/Njun<sub>scrambled</sub>) in each lane (n=3 for each), to remove the fraction of binding that may be non-specific as indicated by Njun<sub>scrambled</sub> binding.

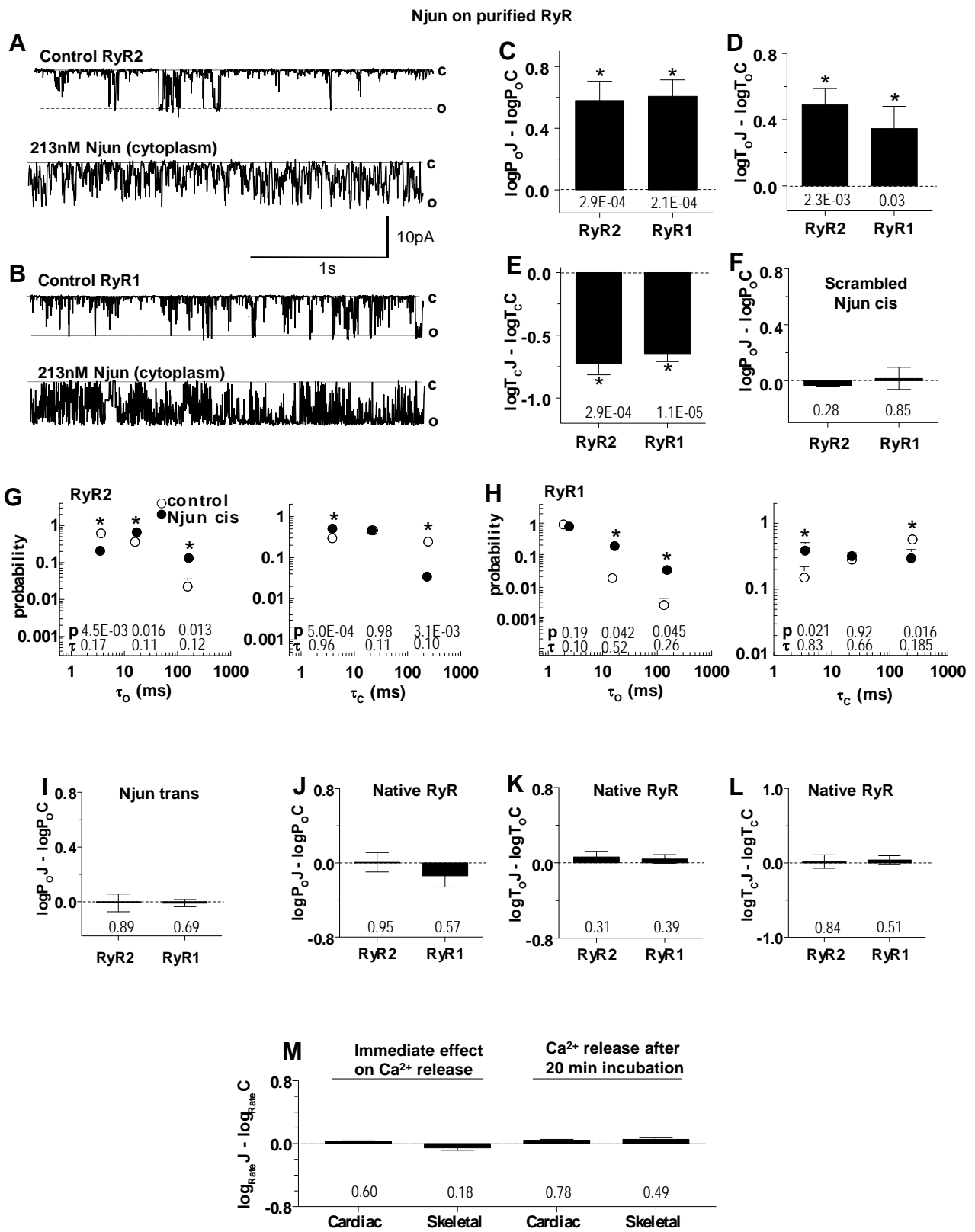
**Fig. 8. A region of junctin that interacts with RyRs.** **A)** Sequence of human junctin with KEKE-like motif residues (86-107) highlighted. **B)** Conservation of the KEKE-like motif sequence in human, canine and rabbit junctin and comparison with the active KEKE motif in skeletal triadin. Rabbit junctin is not fully sequenced, so residue numbers are for the partial sequence (accession #AAF37204) **(C-E).** Effects of the KEKE peptides on average  $\log P_{OJ} - \log P_{OC}$ ,  $\log T_{OJ} - \log T_{OC}$ , and  $\log T_{CJ} - \log T_{CC}$  (defined in Fig. 2 legend) for: rabbit KEKE peptide on the luminal side of RyR2 (n=16) and RyR1 (n=12) (filled bins); canine KEKE peptide (included because Cjun was derived from canine junctin (methods)) on the luminal side of RyR2 (n=4) and RyR1 (n=4) (grey bins); rabbit KEKE peptide on the cytoplasmic side of RyR1 (n=8) and RyR2 (n=8) (clear bins). Asterisk (\*) indicate significant differences between control parameters and parameter with KEKE constructs: p values are given below bins for each construct. **F)** Affinity chromatography showing RyR2 and RyR1 binding to canine KEKE peptide-streptavidin agarose. **G)** Average densitometry data showing consistent binding of RyR1 (n=3) and RyR2 (n=3) to canine KEKE peptide-streptavidin agarose. (\*) indicate ratios significantly greater than zero: p values are given under bins.

Figure 1

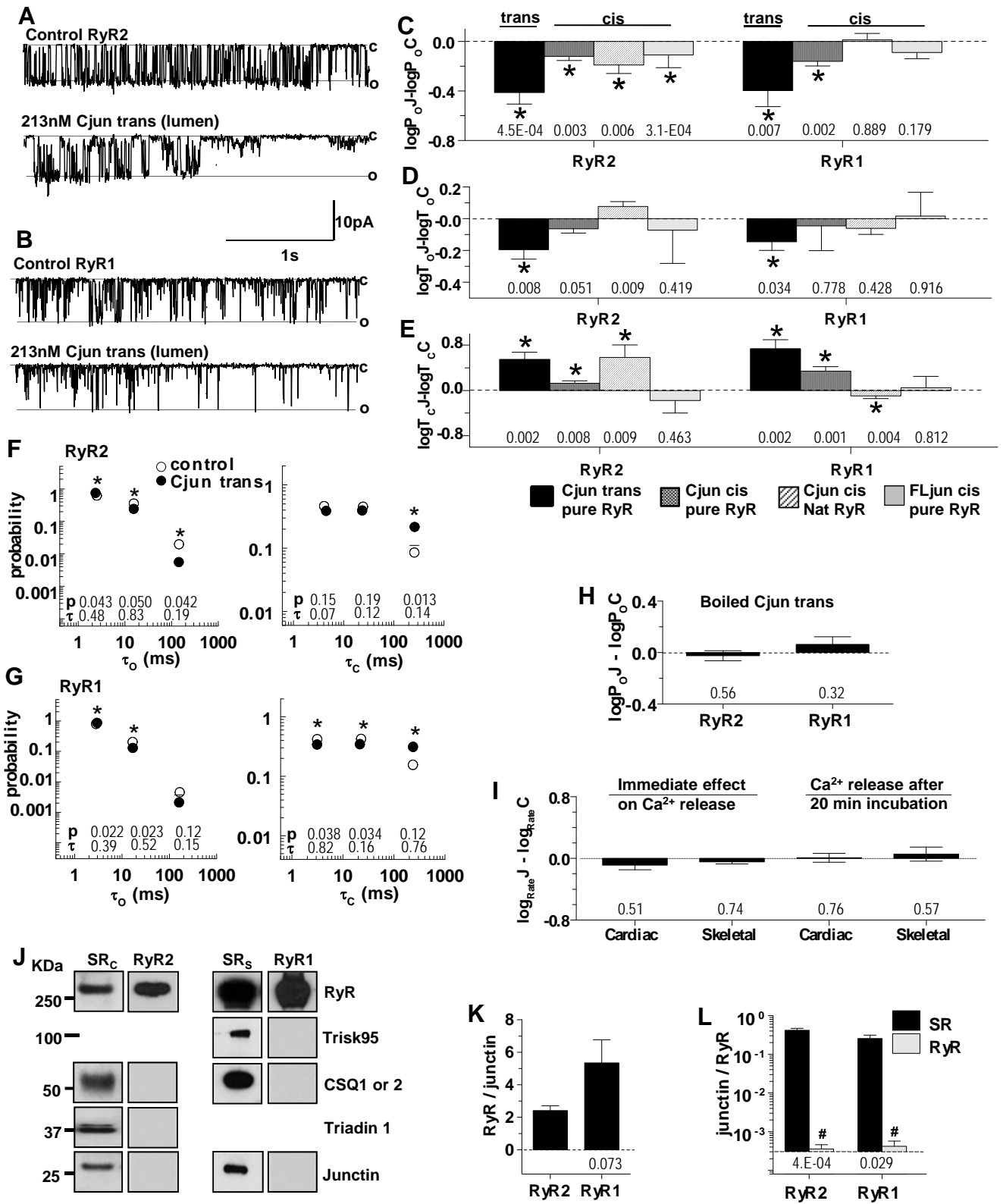


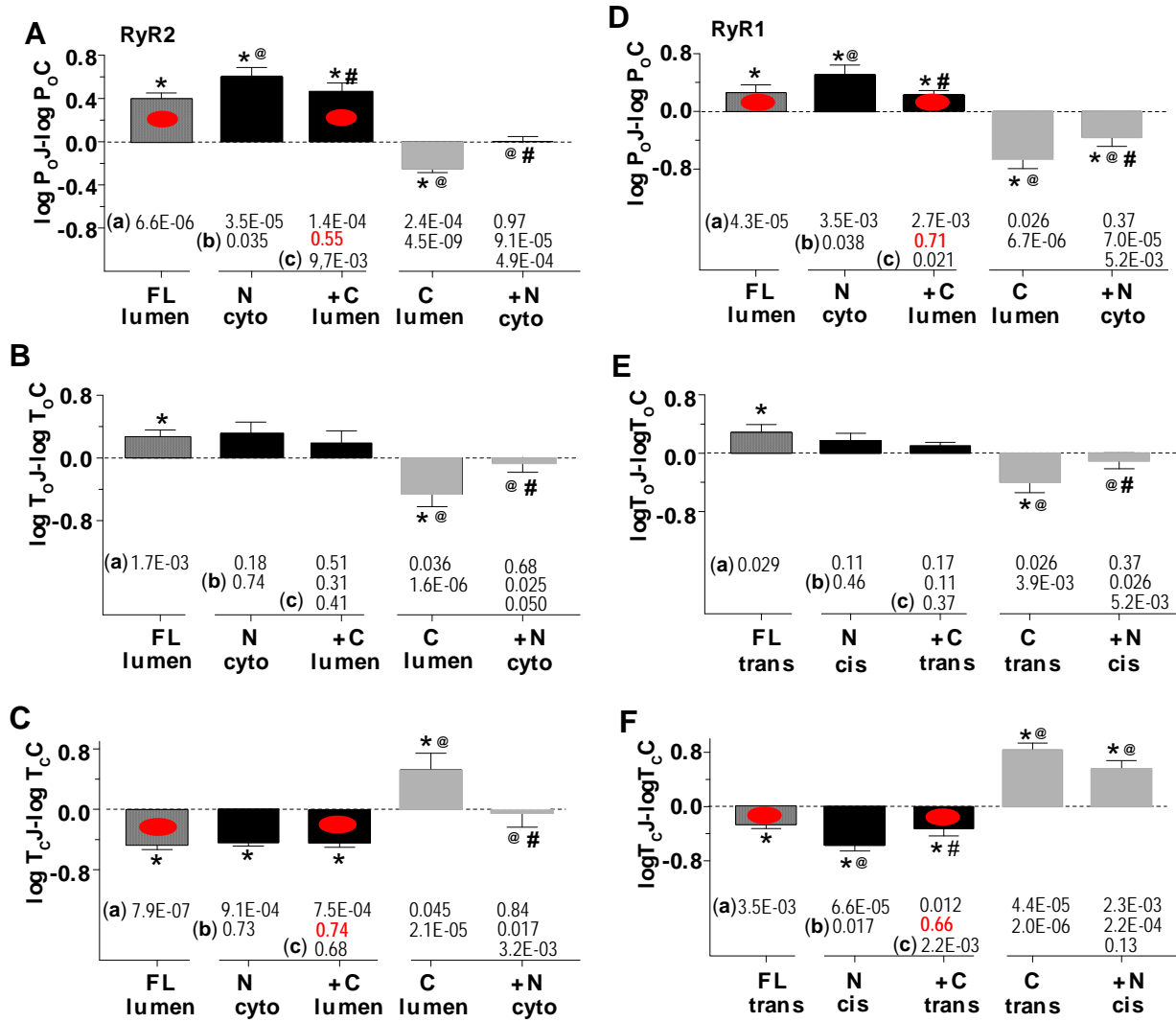
FLjun on purified RyR

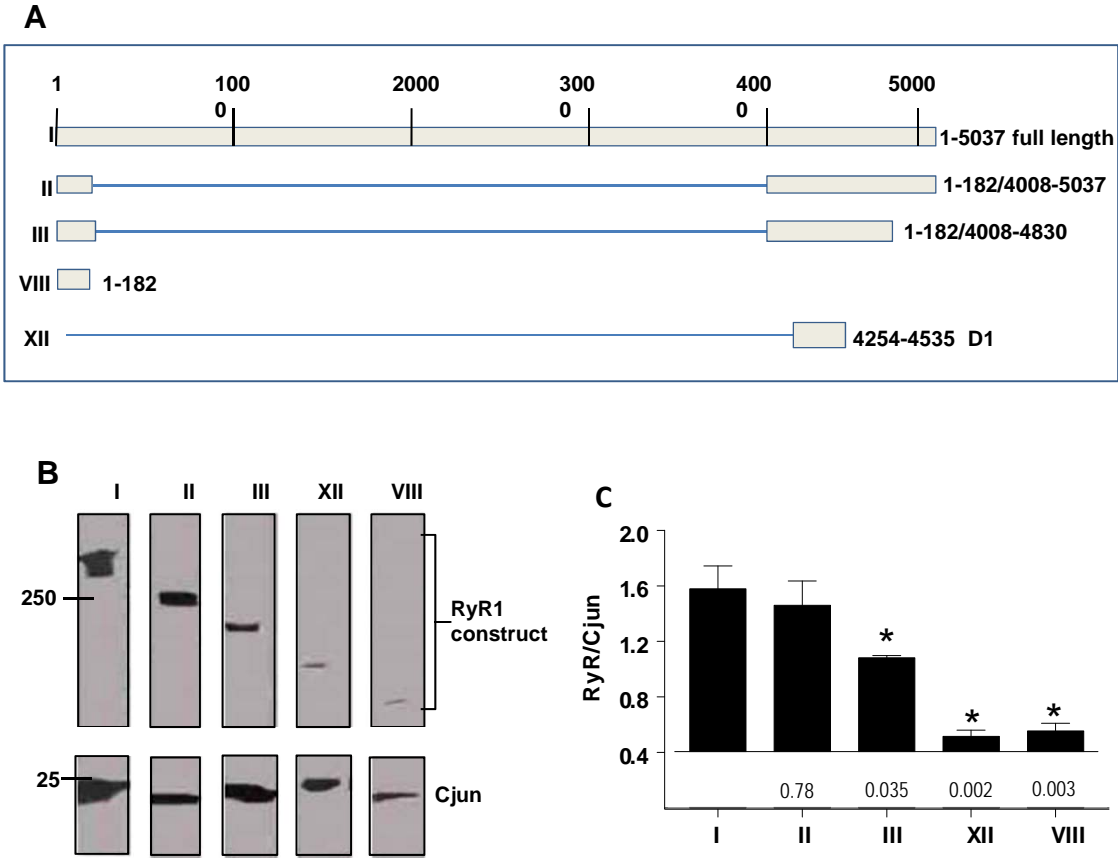


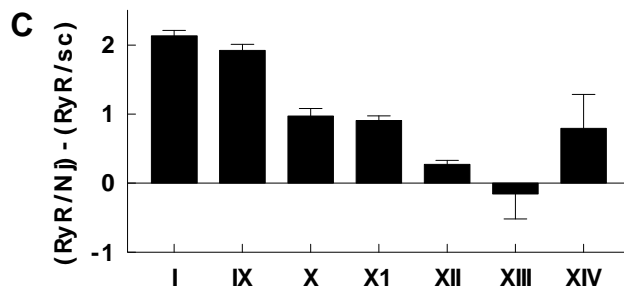
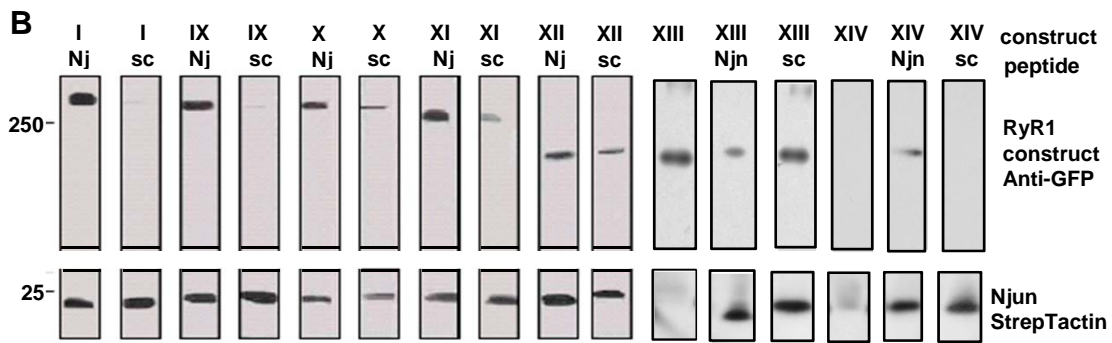
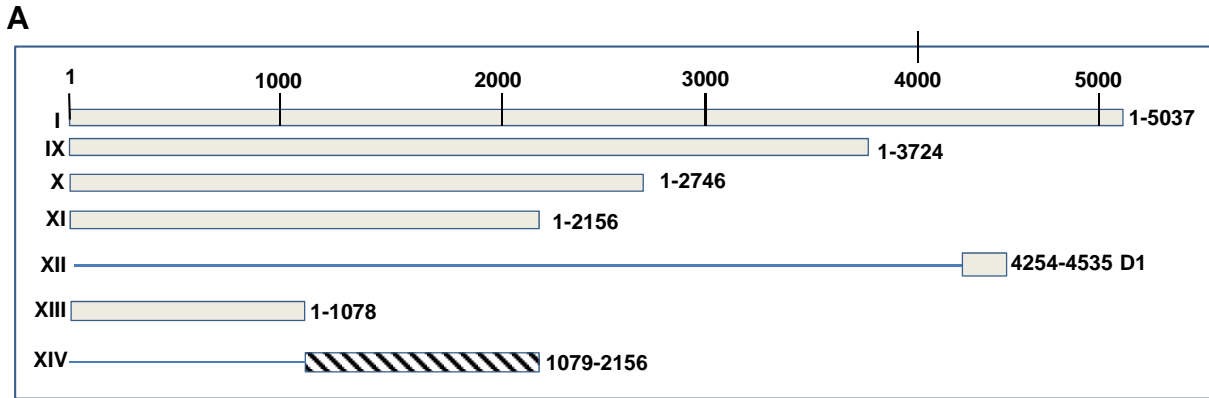


Cjun on purified RyR









**A**

<sup>1</sup>MAEDKETKHGGHKNRKGGLSGTSFFTFWMVIALLGWVTSVAVVEFDLVDYEEVLGKLGIDADGGDFDVEDDAKVLLEG<sup>80</sup>  
<sup>81</sup>PSGVAKRRTKAKVKELTKEELKKEKEKPESRKESKNEERKKGKKEDVRKDKKIADADLSRKESPKGKKDREKEKVDLEKS<sup>160</sup>  
<sup>161</sup>AKTKENRKKSTNMKDVSSKMASRDKDRKESRSSTRYAHLTKGNTQKRNG<sup>210</sup>

**B**

**Cjun<sub>KEKE</sub>Human:** <sup>86</sup>KRRTKAKVKELTKEELKKEKEK<sup>107</sup>  
**Cjun<sub>KEKE</sub>Ecanine:** <sup>84</sup>KRRTKAKVKELTKEELKKEKEK<sup>105</sup>  
**Cjun<sub>KEKE</sub>Rabbit:** <sup>53</sup>KRRTKAKVKELIKEELKKGKEK<sup>74</sup>  
**Trisk 95<sub>200-232</sub>:** <sup>200</sup>KTVTKEEKARTKEIEEKTKEVKGVKQEKV<sup>232</sup>

